Malaya Journal of Matematik, Vol. 8, No. 3, 1337-1345, 2020

https://doi.org/10.26637/MJM0803/0106

MHD, Nonlinear thermal radiation and non-uniform heat source/sink effect on Williamson nanofluid over an inclined stretching sheet

T. Srinivasulu[1]* and Shankar Bandari[2]

Abstract

In this article, we have deliberate the impact of non-linear thermal radiation and non-uniform heat source/sink on MHD boundary layer flow of Williamson nanofluid above an inclined stretching surface. Using the similarity transformations, the governing PDE's equations of this problem, are converted into ODE'S. The changed ODE'S with boundary conditions are solved numerically by using RK scheme with shooting technique. The effect of governing parameters on dimensionless flow distributions are plotted and examined. The Numerical outcomes for skin friction, Nusselt number, and Sherwood number are tabulated for various values of physical parameters. It is obtained that temperature increases with enhance in non-uniform heat source and velocity profile diminishes with increase in an angle of inclination.

Keywords

Williamson nanofluid, MHD, Inclined stretching sheet, Non-uniform heat source/sink, RK Scheme.

AMS Subject Classification

76X05.

[1] *Department of Mathematics, Government Degree College, Hayathnagar-501505, Telangana, India.*

[2] *Department of Mathematics, Osmania University, Hyderabad-500007, India.*

***Corresponding author**: [1] mailtsvs@gmail.com; [2]bandarishanker@yahoo.co.in

Article History: Received **24** April **2020**; Accepted **19** August **2020**

Contents

Nomenclature

$B_\circ$	Magnetic field
T_∞	Ambient fluid temperature
Rd	Radiation parameter
C_∞	Ambient fluid concentration
u	Velocity component along $x-$axis
v	Velocity component along $y-$axis
u_w	Velocity component at the wall
v_w	Velocity component at the wall
ν	Kinematic viscosity
ρ_f	Density of fluid
γ	Angle of inclination
σ	Electrical conductivity
D_B	Brownian diffusion coefficient
D_T	Thermophoresis diffusion coefficient
$\tau = \frac{(\rho c)_\rho}{(\rho c)_f}$	The ratio between the effective heat capacity of nanoparticle material and heat capacity of the fluid
K	Thermal conductivity
$\alpha = \frac{K}{\rho c_p}$	Thermal diffusivity
M	Magnetic parameter
Pr	Prandtl number
Nt	Thermophoresis parameter
Nb	Brownian motion parameter
Le	Lewis number
λ_1	Williamson parameter
$\mu_\circ$	limiting viscosity at zero shear rate
μ_∞	limiting viscosity at infinite shear rate
I	Identity vector
P	Pressure
τ_1	Extra stress tensor

π	Second invariant strain tensor
A_1	First Rivlin-Erickson tensor

1. Introduction

Nanofluid is an innovative class of fluid that includes nano-sized particles in a low thermal conductivity base fluid such as ethylene glycol and water, to improve its thermal conductivity and in general the nanoparticles are metal or metal oxide, increases the conduction and convection coefficient. This particles allows more heat transfer out of the coolant (Choi and Eastman[1]). It looks that the term nanofluid was first presented by Choi et al.[1] and later it was adopted by many researcher. Nanofluids are plays an important role in thermal engineering, material science, medical applications, biomedical industry, solid state lighting, micro-electronics and transportations. Mohammed Amin Makaram et al.[2] have deliberated heat and mass transfer flow in various nanofluids. Hayat et al.[3] consider the model of MHD joule heating flow of nanofluid. MHD thermal radiation effect on Carreau nanofluid over a shrinking sheet is investigated numerically by Bhatti et al.Mohammad16. MHD flow over a permeable stretching sheet in the presence of nanoparticles is examined by Sandeep et al.[5] by using bvp4c with MATLAB program. The Nusselt number of the nanofluid was 14% more than that of pure water.

The impact of magnetic field has a extensive range of applications in MHD generators, MHD pumps, engineering, medicine and physics. Bakr [6] examined the MHD effect on micropolar fluid in the presence of nanoparticles over a semi-infinite vertical porous plate. The nanoparticles are not transported in the magnetic field. Due to this cause, temperature and nanoparticle volume fraction are enhanced. Krisnedu Bhattacharya et al. [7] are discussed the cause of MHD heat transfer flow over a exponentially stretching permeable stretching sheet in existence of nanoparticles. Shankar et al. [8] examined the numerically unsteady heat and mass transfer flow of MHD nanofluid along stretching sheet with effect of non-uniform heat source/sink by using Keller box method. Amount of local skin friction increases with increase in magnetic parameter. Recently Waqas et al.[9] explored transport of nanoparticles containing microorganisms in the presence of bio convective flow of magnetic field in a stratified medium.

On the other hand, non-Newtonian fluids play important character in industrial processing and many engineering practical applications. Nadeem et al.[14] explored the flow of non-Newtonian Jeffrey fluid in the presence of nanoparticles numerically by using RK-Fehelberg method. Heat and mass transfer impact on Williamson fluid model in a channel with slip conditions investigated by Hayat et al.[15]. In their study observed that behavior of velocity profile opposite in upper and lower half of the channel with Williamson parameter. Hayat et al.[12]talked about the melting heat transfer boundary layer flow of Williamson nanofluid along nonlinear thicked variable surface. Actually Weissenberg number is the ratio of relaxation time of the fluid to the specific process time. Velocity distribution rise for decay of Weissenberg number. MHD heat and mass transfer flow of Williamson fluid in the presence of nanoparticles with chemical reaction and melting heat transfer in porous medium is studied numerically by Krishnamurthy et al. [13]. In their study observed that rate of heat transfer and skin friction coefficient for Williamson fluid in the absence of nanoparticles is less than that in presence. Ramesh et al. [17]have discussed numerically, the influence of non-linear thermal radiation flow of nanofluid over a riga plate. High temperature for larger values of radiation parameter and temperature ratio parameter. Archana et al. [18]examine the non-linear thermal radiation effect on casson fluid in the incidence of nanoparticles over a wedge by using RK method with shooting technique. The space dependent heat source and temperature dependent source impacts on MHD flow of nanofluid over an non linear stretching surface is investigated numerically by Mahantesh [19]. The change in the space and temperature dependent parameters decreases the temperature.

The flow over a stretching surface has wide range of applications in industries and many engineering processes such as glass fiber manufacture, aerodynamic, rubber sheets, manufacture of plastic, cooling of huge metallic plate and wire drawing. Ramesh et al.[20] reported influence of non-uniform heat source on MHD dust heat transfer flow over an inclined stretching sheet and investigated respective governing factors effect on temperature, velocity and concentration distribution. Suction, heat generation and MHD impact on nanofluid over an inclined stretching sheet with mixed convection by Pragya et al.[21].Heat transfer of MHD flow over an inclined past stretching sheet is studied by Mohammad Ali et al. [22]. Prabhakar et al. [23] have numerically considered the impact of Lorerntz force on tangent hyperbolic flow over a stretching sheet in the presence of nanoparticles. Magnetic field's impact on 3D Maxwell flow over an inclined stretching sheet is investigated by Ahamad M.Abdal Hadi [24].

Above literature survey motivates the present study, the main objective to analyze the effect of non-linear thermal radiation, non-uniform heat source and MHD flow of Williamson nanofluid over an inclined stretching sheet, which is play vital role in the view of engineering purposes.

2. Mathematical formulation

We consider a 2-dimensional flow of Williamson nanofluid which is steady, viscous and incompressible fluid, over an inclined linear stretching sheet. Consider a coordinate system so that the flow is being confined next to x-axis and y-axis is normal to the stretching sheet. Stretching sheet make an angle of γ with the positive direction of x-axis. Let the stretching sheet velocity $u = u_w = ax$ (a is positive). Apply the magnetic field, non-uniform heat source and nonlinear thermal radiation along normal to the x-axis. The wall temperature and nano particle volume faction are T_w (ambient fluid temperature) and c_w (concentration) respectively. Assume that the produced magnetic field is much smaller than the applied magnetic field,

and is ignored.

Fluid Model: Williamson fluid model taken by Nadeem [11] is considered. To the current model of fluid, the Cauchy stress tensor S is defined as;

$$S = -PI + \tau_1$$
$$S = -PI = A_1(\mu_\infty + \frac{\mu_0 - \mu_\infty}{1-\Gamma\dot{\gamma}})$$

Where $\Gamma > 0$ is a time constant and $\dot{\gamma}$ is considered to be

$\dot{\gamma} = \sqrt{\frac{\pi}{2}}$, $\pi = trace(A_1^2)$

We considered only for the case

$\mu_\infty = 0$ and $\Gamma\dot{\gamma} < 0$.

Then, we obtain

$\tau_1 = [\mu_0 A_1(1-\Gamma\dot{\gamma})^{-1}]$ or $\tau_1 = [\mu_0 A_1(1+\Gamma\dot{\gamma})]$

The equation of conservation of momentum , thermal energy and nanoparticle concentration including MHD, non-uniform heat source /sink and nonlinear thermal radiation are written as follows [16].

$$\frac{\partial u}{\partial x} + \frac{\partial v}{\partial y} = 0 \tag{2.1}$$

$$u\frac{\partial u}{\partial x} + v\frac{\partial u}{\partial y} = v\frac{\partial^2 u}{\partial y^2} + \sqrt{2}\Gamma v\frac{\partial u}{\partial y}\frac{\partial^2 u}{\partial y^2} + g\beta_1(T-T_\infty)\cos(\gamma) + g\beta_1^*(C-C_\infty)\cos(\gamma) - \frac{\sigma B_0^2 u}{\rho_f} \tag{2.2}$$

$$u\frac{\partial T}{\partial x} + v\frac{\partial T}{\partial y} = \alpha\frac{\partial^2 T}{\partial y^2} + \tau[D_B\frac{\partial C}{\partial y}\frac{\partial T}{\partial y} + \frac{D_T}{T_\infty}(\frac{\partial T}{\partial y})^2] + \frac{q'''}{\rho c_P} - \frac{1}{\rho c_P}\frac{\partial q_r}{\partial y} \tag{2.3}$$

$$u\frac{\partial C}{\partial x} + v\frac{\partial C}{\partial y} = D_B\frac{\partial^2 C}{\partial y^2} + \frac{D_T}{T_\infty}(\frac{\partial^2 T}{\partial y^2}) \tag{2.4}$$

The appropriate boundary conditions are

$$y \longrightarrow 0 : u = u_w = ax, v = v_w, T = T_w, C = C_w$$
$$y \longrightarrow \infty : u = 0, T = T_\infty, C = C_\infty. \tag{2.5}$$

Introduce the corresponding similarity transformations

$$\eta = y\sqrt{\frac{a}{v}}, \psi = \sqrt{av}xf(\eta),$$
$$\theta(\eta) = \frac{T-T_\infty}{T_w - T_\infty}, \phi(\eta) = \frac{C-C_\infty}{C_w - C_\infty}. \tag{2.6}$$

The stream function ψ defined as $u = \frac{\partial\varphi}{\partial y}$ and $v = -\frac{\partial\varphi}{\partial y}$. $f(\eta), g(\eta)$ and $\phi(\eta)$ are dimensionless stream function, dimensionless temperature function, and dimensionless concentration functions respectively. The dimensionless form of $q'''$is as follows (Abdul Hakeem(2014)):

$$q''' = \frac{ku_w}{xv}[A^*(T_w - T_\infty)f' + B^*(T-T_\infty)]$$

Where A^* is space dependent and B^* is the temperature dependent internal heat source/sink factors respectively. Such two parameters are positive and therefore reflect internal heat generation and negative internal heat absorption. The estimate for Rosseland given a(1931) gives radiative heat flux term q_r is of the form, $q_r = -\frac{4\sigma^*}{3k^*}\frac{\partial T^4}{\partial y}$ and T^4 can be spelled as $T^4 = [1+\theta\theta_w - \theta]^4 T_\infty^4$ where $\theta_w = \frac{T_w}{T_\infty}$ is temperature ratio parameter(Shehzad et al.2014).

Use (2.5) and (2.6) in the governing equations (2.2)-(2.4), we obtain the ODE's as follows:

$$f'''(1+\lambda_1 f'') + ff'' - (f')^2 + Gr\theta\cos(\gamma) + Gm\phi\cos(\gamma) - Mf' = 0 \tag{2.7}$$

$$[1+\frac{4}{3}Rd(1+\theta\theta_w-\theta)^3]\theta'' + 4Rd(1+\theta\theta_w-\theta)^2(\theta_w-1)(\theta')^2 + Pr(Nb\theta'\phi' + \theta' f + Nt(\theta')^2) = -(A^* f' + B^*\theta) \tag{2.8}$$

$$\phi'' + Le(f\phi') + \frac{Nt}{Nb}\theta'' = 0 \tag{2.9}$$

The associative boundary conditions becomes

$$\text{At} \quad y = 0 : f'(y) = 1, f(y) = S, \theta(y) = 1, \phi(y) = 1,$$
$$\text{At} \quad y \to \infty : \quad f'(y) = 0, \theta(y) = 0, \phi(y) = 0 \tag{2.10}$$

Where the governing parameters defined as:

$$M = \frac{\sigma B_0^2}{\rho_f a}, \lambda_1 = \sqrt{\frac{2a}{v}}ax\Gamma, Le = \frac{v}{D_B}, Gr = \frac{g\beta_1(T-T_\infty)}{a^2 x},$$
$$Gm = \frac{g\beta_1^*(C-C_\infty)}{a^2 x}, Pr = \frac{v}{\alpha}, Nb = \frac{\tau D_B(C_w - C_\infty)}{v},$$
$$Nt = \frac{\tau D_T(T_f - C_\infty)}{T_\infty v}, Rd = -\frac{4\sigma^* T_\infty^3}{kk^*} \tag{2.11}$$

The physical quantities, skin friction coefficient (Cf_x), the local Nusselt number (Nu_x) and local Sherwood number (Sh_x) are defined below :

$$Cf_x = \frac{\tau_w}{\rho u_w^2}, Nu_x = \frac{xq_w}{k(T_w - T_\infty)}, Sh_x = \frac{xq_m}{D_B(C_w - C_\infty)}. \tag{2.12}$$

At the surface, the shear stress, heat and mass fluxes are

$$\tau_w = \mu[\frac{\partial u}{\partial y} + \frac{\Gamma}{2^{\frac{1}{2}}}(\frac{\partial u}{\partial y})^2],$$
$$q_w = -k(\frac{\partial T}{\partial y})_{y=0} + (q_r)_{y=0}, q_m = -D_B(\frac{\partial C}{\partial y})_{y=0}. \tag{2.13}$$

We are provided with (2.6) substitute equations in (2.12) and (2.13)

$$Re_x^{1/2} Cf_x = (1 + \frac{\lambda_1}{2} f''(0)) f''(0),$$
$$Re_x^{-1/2} Nu_x = -(1 + \frac{4}{3} Rd\theta_w^3)\theta'(0), \tag{2.14}$$
$$Re_x^{-1/2} Sh_x = -\phi'(0).$$

through where $Re_x = \frac{u_w x}{\nu}$ is the local Reynolds number.

3. Numerical Method

With boundary conditions (2.10), the non-linear ODE (2.7)–(2.9) is numerically by RK method with shooting technique. Steps:

- Reduce the OD eqs to a set of simultaneous ordinary equations.
- Find out the three unknown initial conditions $f''(\eta), \theta(\eta), \phi(\eta)$ at $\eta = 0$ with shooting technique and given initial conditions.
- By taking the initial values, Boundary value problem (BVP) is turned to an initial value problem(IVP).
- The resultant IVP is solved iteratively using RK method.

4. Result and discussions

With boundary conditions (2.10), the set of non-linear ODEs (2.7), (2.8) and (2.9), with are solved numerically by RK method and using shooting technique. Table1. Array the assessment of the data produced by the current method with Wang [2].The result shows excellent agreement. Table 2: shows the variation of $-f''(0)$, $-\theta'(0)$ and $-\phi'(0)$ for diverse values of a parameter λ_1, γ, M, Nb, Nt, Pr, Rd, Gr, Gm, A^*, B^*, S, θ_w and Le.

Fig.1 portrays the impact of magnetic parameter M on the flow fields for different values of M. An electrically conducting fluid in the occurrence of magnetic field produces a force, it is resist the flow, due to this cause, decrease the velocity curves, rise in the temperature and as well as concentration profile. Fig.2 expresses the outcome of angle of inclination on temperature and concentration profile for several values of angle of inclination. We can see that velocity curves decrease and temperature, concentration distribution are enhances with enhance in an angle of inclination because

Table 1. Contrast the values of $-\theta'(0)$ when $M = Nb = Nt = Le = \lambda_1 = A^* = B^* = Gr = Gm = S = \theta_w = Rd = 0$ and $\gamma = 0^\circ$

Pr	$Wang(10)$	$Present$
0.2	0.1691	0.196549
0.7	0.4539	0.454442
2.0	0.9114	0.911340
7.0	1.8954	1.895364

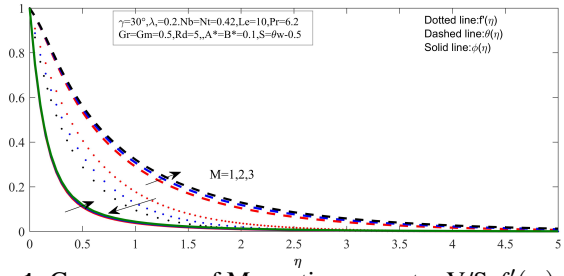

Figure 1. Consequence of Magnetic parameter V/S $f'(\eta)$, $\theta(\eta)$, $\phi(\eta)$.

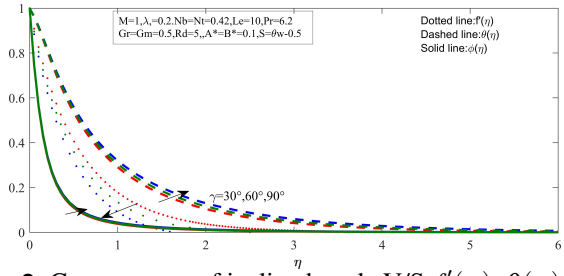

Figure 2. Consequence of inclined angle V/S $f'(\eta)$, $\theta(\eta)$, $\phi(\eta)$.

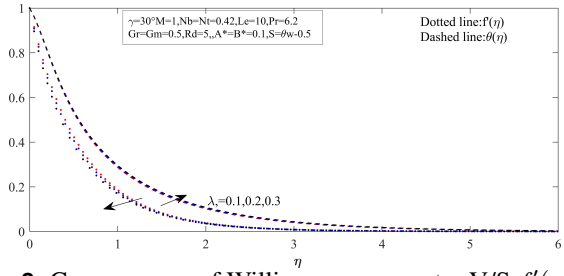

Figure 3. Consequence of Williamson parameter V/S $f'(\eta)$, $\theta(\eta)$.

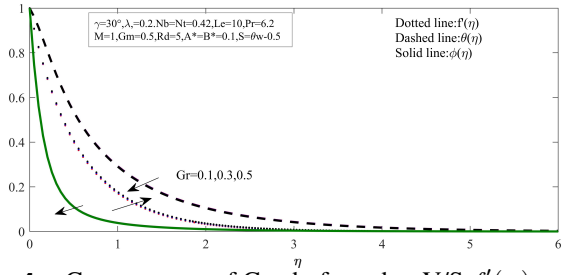

Figure 4. : Consequence of Grashof number V/S $f'(\eta)$, $\theta(\eta)$, $\phi(\eta)$.

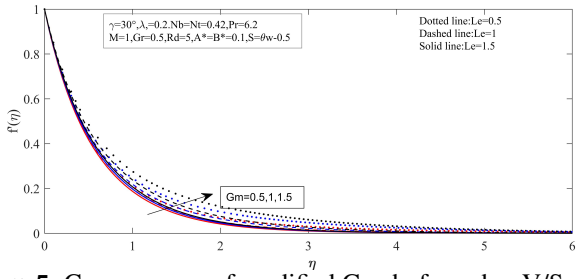

Figure 5. Consequence of modified Grashof number V/S $f'(\eta)$.

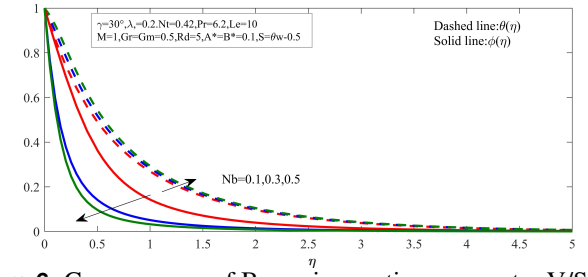

Figure 6. Consequence of Brownian motion parameter V/S $\theta(\eta)$, $\phi(\eta)$.

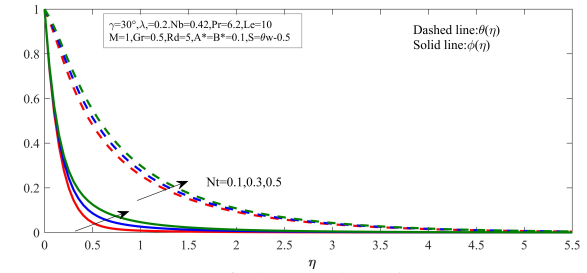

Figure 7. Consequence of Thermophoresis parameter V/S $\theta(\eta)$, $\phi(\eta)$.

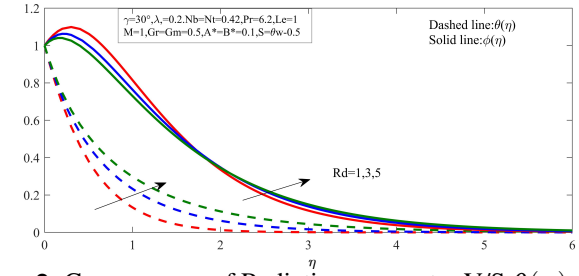

Figure 8. Consequence of Radiation parameter V/S $\theta(\eta)$, $\phi(\eta)$.

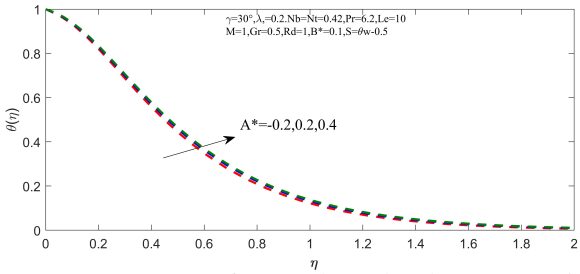

Figure 9. Consequence of Space dependent heat source/sink parameter V/S $\theta(\eta)$.

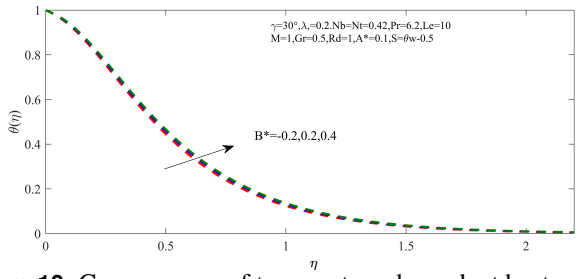

Figure 10. Consequence of temperature dependent heat source/sink parameter V/S $\theta(\eta)$.

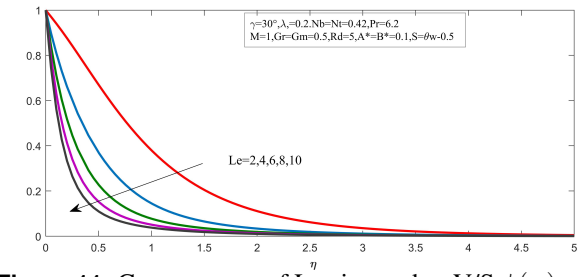

Figure 11. Consequence of Lewis number V/S $\phi(\eta)$.

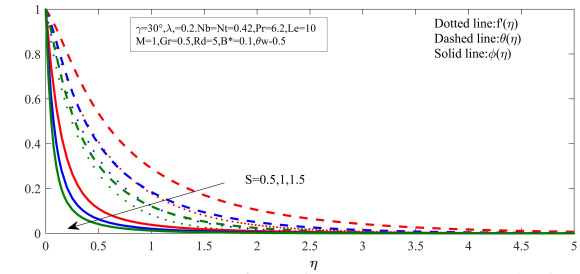

Figure 12. Consequence of Suction parameter on velocity V/S $f'(\eta)$, $\theta(\eta)$, $\phi(\eta)$.

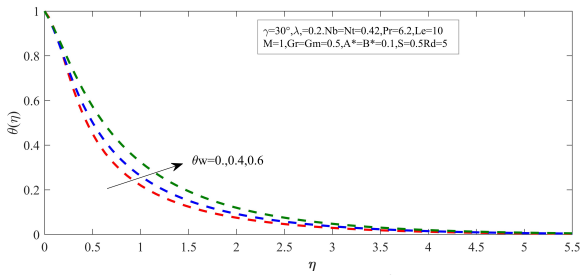

Figure 13. Consequence temperature ratio parameter V/S $\theta(\eta)$.

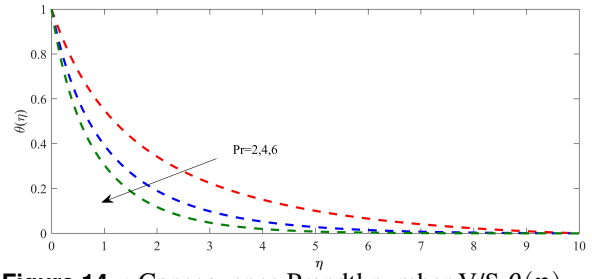

Figure 14. : Consequence Prandtl number V/S $\theta(\eta)$.

of buoyancy force. Flow is high effected in the nonexistence of an angle of inclination compare to presence of an angle of inclination.

Fig.3 reveals the impact of Williamson factor on the velocity and temperature curves. It can be observed that velocity reduces the hike in Williamson parameter λ_1. Because after increasing Williamson parametric quantity the fluid proposes more defiance to flow which contracting velocity profile, it also leads to raise the temperature distribution. Fig.4 shows the graph of velocity, temperature and concentration distributions for several values of Grashof number. We observed that, if Grashof number is increase, the buoyancy force enhance the velocity of the fluid velocity and thickness of the boundary layer, it leads to velocity profile increase. The physical analysis gives that If $Gr < 0$, it designates heating of the boundary layer surface or cooling of the fluid and if $Gr > 0$, it signifies heating of the fluid or cooling of the boundary layer surface, and if $Gr = 0$, correspondence to the non appearance of the free convection current. Because of buoyancy force, temperature and concentration curves are decreases with increase in Grashof number. The graph of velocity distribution for a choice of values of the modified Grashof number with *Le*= 0.5,1 and 1.5 is plotted in Fig.5. It shows velocity profile raises with increase in *Gm*, also mentioned that velocity decrease with increase in *Le* values for fixed *Gm*.

The variations in temperature and concentration profiles for various values of Brownian motion parameter (*Nb*) are addressed in Fig.6. When we rise the values of *Nb*, thermal boundary layer thickness increase and concentration layer thickness is decay because of collision of the nanofluid particles. Fig.7 represents the outcome of thermophoresis parameter (*Nt*) on temperature and concentration outline for varied values of *Nt*. Increase the values of *Nt*, nanoparticles move from hotter region to colder area because of thermophoretic force is enhance, which leads to nanoparticle volume fraction and temperature increase.

Fig.8 indicates the effect on temperature and concentration distribution of radiation parameter (*Rd*). Increase the values of *Rd* provides more heat to the fluid, which leads to enhance the thermal boundary layer thickness, temperature and concentration profiles. The result of A^* on temperature and concentration curves are plotted in Fig.9. A^* act as a heat generator if $A^* > 0$ and heat absorption if $A^* < 0$. Heat source help to enhance the thermal boundary layer thickness and heat absorption decrease the thermal boundary layer thickness. The impact of temperature dependent heat source/sink parameter (B^*) on temperature profile is plotted in Fig.10. If B^* is positive, which released energy and it leads to enhance the temperature profile and B^* is negative, provides energy is absorbed and this leads to temperature dropped.

Fig.11 shows the concentration profile for various estimates of Lewis Number (*Le*). Concentration profile diminishes with gain in *Le*. *Le* is dependent on the Brownian diffusion coefficient. The larger values of Le leads to weaker Brownian diffusion coefficient. Thus concentration profile diminishes with increase in *Le*. Fig .12 describes the outcome of suction factor on velocity, temperature and concentration profiles. Due to imposition wall suction the fluid is brought closer to the sheet and it reduces the momentum boundary layer thickness, thermal boundary layer thickness and nano particle volume fraction. These causes the velocity, temperature and concentration profiles decrease.

Fig.13 shows the impact of temperature ratio constraint (θ_w) on temperature curves for various values of θ_w,θ_w is the ratio of temperature of the fluid at the wall to the free surface temperature of the fluid. $\theta_w > 1$ means wall temperature exceeds the free surface temperature of the fluid and $\theta_w < 1$ means the free surface temperature exceeds the wall temperature of the fluid. An increase of θ_w, result in the temperature profile enhances. The influence of Prandtl number(*Pr*) on temperature profile for various values of *Pr* are reported in Fig.14.*Pr* is the ratio of kinematic viscosity to the thermal diffusivity of the fluid. For larger quantities of *Pr*, have less thermal diffusion. Hence temperature curves decreases with enhances in *Pr*.

5. Conclusion

In this work, MHD ,non-uniform heat source/sink and nonlinear thermal radiation effect on Williamson nanofluid over an inclined stretching sheet is numerically studied by using RK method with shooting technique. Following outcomes getting in our study.

- Velocity profile rises with enhance in *Gr* and *Gm* while decrease in M, γ and λ_1.
- Temperature profile increase with raise in M, γ, *Nb*, *Nt*, A^*, B^*, *Rd* and θ_w while decrease in *Gr*, *Pr* and *S*.

- Concentration distribution increases with increase in M, γ and Nt while decrease in Nb, Le and S.
- Nusselt number gain with enhance in Gr, Gm and Rd while decrease in M, λ_1, Nb, Nt, Pr, A^*, B^*, Le, S and θ_w.
- Sherwood number increases with Gr, Gm, Nb, Pr, A^*, B^*, Le and S while decrease in λ_1, Nt and θ_w.

References

[1] Choi ,S.U.S and Eastman, J.A, Enhancing thermal conductivity of fluids with nanoparticles in Proceeding of ASME, *International journal of Mechanical Engineering congress and Exposition*, san Franscisco, USA, 1995, 12-17.

[2] Mohammad Amon Makarem ,Ali Bakhtyari and Mohammad RezaRahimpour, A numerical investigation on the heat and fluid flow of various nanfluids on a stretching sheet, *Heat transfer Asia*, 2017, 1-19.

[3] Hayat,T.,Waqas,M.,Shehazad,S.A and Alsaedi,A., A model of solar radiation and joule heating in magnetohydrodynamic convevtive flow thixotropic nanofluid, *Journal of Molecular Liquids*, vol.215(2016), 704-710

[4] Mohammad Mubashir Bhatti ,Tehseen Abbas ,Mohammad Mehdi Rashidi and Mohammad El-Sayed Ali. Numerical Simulation of entropy generation with thermal radiation on MHD Carreau nanofluid towards a shrinking sheet Entropy. 18(2016).

[5] Sandeep Naramgiri and Sulochana,c., MHD flow over a permeable stretchin/shrinking sheet of a nanofluid with suction/injection, *Alexandia Engineering Journal*, 55(2016), 819-827.

[6] Bakr ,A.A, Effect of chemical reaction on MHD free convection and mass transfer flow of a micropolar fluid with oscillatory plate velocity and constant heat source in a rotating frame of reference, *Commun Nonlinear Sci Numer Simulat.*, 16(2011), 698-710.

[7] Krishnendu Bhatachaarya and Layak,G.C, Magnetohydrodynamic boundary layer flow of nanofluid over an exponentially stretching permeable sheet, *Physicks Research International*, 2014.

[8] Shankar Bandari and Yohannes Yirga ,Unsteady heat anf mass transfer in MHD flow of nanofluids over a stretching sheet with a non-uniform heat source/sink, *International Journal of Mathematical, Physical, Nuclear Science and Engineering*, vol.7(12)(2013).

[9] Waqas ,M.,Hayat,T.,Shehzad,S.A, and Alsaedi,A. Transfort of magnetohydrodynamic nanomaterial in as tratified medium considering gyrotactic microorganisms, *Physica. B Physics of Condensed Matter*, 5292018, 33-40.

[10] C.Y.Wang, Free convection on a vertical stretching surface, *J.Appl. Math Mech.(ZAMM)*, 69(1989), 418-420.

[11] S.Nadeem, S.T.Hussain and Changhoon Lee(2013): Flow of a Williamson fluid over a stretching sheet, *Brazilian Journal Chemical Engineering*, 30(3)(2013), pp.619-625

[12] Hayat,T., Gulnaz Bashir, Waqas ,M.and Alsaedi , MHD 2D flow of Williamson nanofluid over an nonlinear variable thicked surface with heattransfer, *Journal of Molecular Liquids*, 223(2016), 836-844.

[13] Krishnamurthy,M.R,Prasannakumara,B.C.,Gireesha,B.J and Ramasubba Reddy Gorla, Effect of chemical reaction on MHD boundary flow and melting heat transfer of Williamson nanofluid in porous medium, *Engineering Science and Technology*, 192016, 53-61.

[14] Nadeem,S.,Rizwan UI Haq and Khan,Z.H, Numerical solution of non-Newtonian flow over a stretching sheet, *Appl Nanosci.*, 4(2014), 625-631.

[15] Hayat,T. and Hina,S. Effect of heat and mass transfer of peristaltic of Williamson fluid in a non-unioform channel, *Int.J.Numer.Mech.Fluids*, 67(2011), 1590-1604.

[16] Nadeem, S. and S.T.hussain, Flow and heat transfer analysis of Williamson nanofluid, *Appl Nanosci.*, 4(2014), 1005-1012. DOI 10.1007/s13204-013-0282-1.

[17] Ramesh,G.K and Gireesha,B.J. Non-Linear radiative flow of nanofluid past a moving/stationary riga plate, *Frontiers in Heat and Mass Transfer(FHMT)*, 9(3)(2017).

[18] Archana M. and Girisha,B.J, ?Numerical exploration of the combined effects of non-linear thermal radiation and variable thermo-physical properties on the flow of casson nanofluid over a wedge, *Multidisplinary Modeling and Material Structure*, 2017.

[19] Mahantesh M.Nandeppanavar, Effect of space and temperature dependent heat source on heat transfer of MHD nanofluid due to non-linear stretching sheet with chemical reaction, *Journal of Nanofluids*, 6(2017), pp.1-7.

[20] Ramesh,G.K,Gireesha,B.J and Bagewadi,C.S, Heat transfer in MHD dusty boundary layer flow over an inclined stretching sheet with non-uniform heat source/sink, *Advance in Mathematical Physics*, 2012, ID,657805.

[21] Pragya and Vasanthakumari,R.V, Mixed convective nanofluid flow over an inclined stretching plate with MHD and effects of suction and internal heat generation, *Annalas of Pure and Applied Mathematics*, 12(2016), 69-83.

[22] Mohammad Ali,Abdul Alim,Md. and Mohammad Shah Alam,Heat transfer boundary layer flow past an inclined stretching sheet in the presence of magnetic field, *International Journal of Advancements in Research and Technology*, 3(2014), 1–09.

[23] Besthapu Prabhakar ,Shankar Bandari and Rizwan UI Haq, ?Impact of inclined Lorentz forces on tangent hyperbolic nanofluid flow with zero normal flux of nanoparticles at the stretching sheet, *Neural Computer and Applications*, 2016, DOI 10.1007/s00521-016-2601-4.

[24] Dr.Ahamad M., Abdal Hadi , Ndhal.M., Abdal Ameer, Effect of magnetic field over an inclined stretching sheet of three dimensional Maxwell fluid in the absence of mixed convection, *Mathematical Theory and Modeling*,

5(13)(2015), 1–10.

⋆⋆⋆⋆⋆⋆⋆⋆⋆
ISSN(P):2319 – 3786
Malaya Journal of Matematik
ISSN(O):2321 – 5666
⋆⋆⋆⋆⋆⋆⋆⋆⋆

Table 2. Enumerate the values of $-f''(0)$, $-\theta'(0)$ and $-\phi'(0)$ for various values of parameters.

M	γ	λ_1	Gr	Gm	Nb	Nt	Pr	Rd	A^*	B^*	Le	S	θ_w	$-f''(0)$	$-\theta'(0)$	$-\phi'(0)$
1	30°	0.2	0.5	0.5	0.4	0.4	6.2	5	0.1	0.1	10	0.5	0.5	1.9222	0.7075	5.5774
2														2.4049	0.6835	5.7177
3														2.8742	0.6652	5.6707
	0°													1.5743	0.7252	5.8197
	30°													1.9222	0.7075	5.7744
	45°													1.7632	0.7167	5.7944
		0.1												1.7538	0.7130	5.7901
		0.2												1.9222	0.7075	5.7744
		0.3												2.2583	0.7001	5.7513
			0.1											1.9618	0.7048	5.7688
			0.3											1.9419	0.7062	5.7716
			0.5											1.9222	0.7075	5.7744
				0.1										1.9379	0.7070	5.7729
				0.3										1.9301	0.7072	5.7737
				0.5										1.9222	0.7075	5.7744
					0.1									1.9081	1.4754	1.7540
					0.3									1.9213	0.9138	5.3921
					0.5									1.9225	0.5422	5.9718
						0.1								1.9291	0.9440	6.0070
						0.3								1.9245	0.7779	5.8247
						0.5								1.9201	0.6444	5.7447
							5							1.9192	0.7231	5.7395
							10							1.9277	0.5644	5.9510
							15							1.9308	0.3583	6.1724
								1						1.9302	0.4271	6.0870
								3						1.9260	0.6076	5.8922
								5						1.9222	0.7075	5.7744
									0.1					1.9222	0.7075	5.7744
									0.2					1.9221	0.6955	5.7845
									0.3					1.7410	5.5400	10.1708
										0.1				1.9222	0.7075	5.7744
										0.2				1.9219	0.6915	5.7874
										0.3				1.9216	0.6751	5.8007
											1			1.8616	1.5957	0.5566
											5			1.9094	0.8948	2.7720
											10			1.9222	0.7075	5.7744
												-0.5		1.1954	0.0592	0.2250
												0		1.5119	0.3398	2.1945
												0.5		1.9222	0.7075	5.7744
													1	1.9276	0.4416	6.0808
													2	1.9268	0.5099	6.0091
													3	1.9256	0.5952	5.9164